Manifestation of Strongly Delocalized Atomic States in the 5*s* Photoionization of Xenon

H. Schmoranzer, S. Lauer, and F. Vollweiler
Fachbereich Physik, Universität Kaiserslautern, D-67653 Kaiserslautern, Germany

G. Reichardt
BESSY, Lentzeallee 100, D-14195 Berlin, Germany

K.-H. Schartner, G. Mentzel, and O. Wilhelmi
I. Physikalisches Institut, Justus-Liebig-Universität, D-35392 Giessen, Germany

V. L. Sukhorukov, B. M. Lagutin, and I. D. Petrov
Rostov State University of Transport Communications, RUS-344038 Rostov-on-Don, Russia
(Received 30 May 1997)

The photoionization (PI) of the Xe atom was investigated in the vicinity of the 5*s*-shell threshold by photon-induced fluorescence spectroscopy. The highest resolution so far attained of 2 meV enabled us to observe a new series of resonance structures in the 5*s*-PI cross section closely above threshold. Calculations of the partial 5*s*- and 5*p*-PI cross sections were performed taking into account many-electron correlations. These structures were related with strongly delocalized *f*-resonances which affect the 5*s*-PI cross section due to their mixing with *p*-resonances. [S0031-9007(97)04758-3]

PACS numbers: 32.80.Dz, 31.25.Jf, 32.80.Fb

Many atomic properties are connected with the unoccupied atomic states. In the calculations of, e.g., the atomic polarizability or the van der Waals forces, the summation over all virtual states is involved [1]. Consequently, the spatial distribution of each virtual state is important, and it is interesting to study differently localized excited atomic states in such physical phenomena where they manifest themselves individually. The *ns* subvalence shell photoionization of the rare-gas atoms is one of these phenomena because the partial *ns*-photoionization cross section has resonance character associated with doubly excited atomic states [2].

Although the resonance structures in the partial *ns*-photoionization cross section near threshold have been observed almost a decade ago [2], only a few papers [3–5] until now have dealt with cross section calculations accounting for the doubly excited states. The calculation performed in our previous work [4,5] for the 4*s* photoionization of the Kr atom includes only $4p^4\,nd\,n'p$ doubly excited states, i.e., only those atomic states which contain the localized excited nd and $n'p$ electrons. Doubly excited states where one of the excited electrons is strongly delocalized, namely $n'f$, have been discussed in [6] but were not assigned to the experimental resonance structures. The dynamics of the influence of such states on the cross section remained unclear because the $n'f$ electrons have a very small probability density inside the atomic core. Thus, the main goal of the present paper is the experimental and theoretical study of the photoionization processes affected by strongly delocalized states.

The 5*s* photoionization of the Xe atom was chosen in the present case because a preliminary estimate of the energy of the $5p^4\,ndn'f$ states by means of the hydrogenlike $(1/n^2)$ formula showed that there are four close lying doubly excited states, namely $5p^4(^3P)\,5d\,^4D_{5/2,7/2}$-$5f_{5/2,7/2}$, immediately above the 5*s* threshold which are particularly suited for a high-resolution measurement by means of the photon-induced fluorescence spectroscopy (PIFS) technique developed over the years [2,7,8]. All these states having total angular momentum $J = 1$ can in principle be detected in a photoabsorption experiment. However, these states were not found in the measurements of the total photoabsorption cross section [6] as well as of the partial photoionization cross sections [9,10]. Therefore in the present study a PIFS measurement at the highest resolution yet obtained was performed to determine the exciting-photon energy dependence of the 5*s*-photoionization cross section σ_{5s} in the threshold region. The energy resolution in these measurements is solely determined by the bandwidth of the exciting radiation. The spectral resolution of the fluorescence radiation must be chosen only sufficient to uniquely separate the fluorescence from different excited states. In parallel the σ_{5s} values in the 5*s*-threshold region were calculated.

The experimental setup used for the present measurement is based on a previous one [7,8,11,12]. Synchrotron radiation from the electron storage ring BESSY, Berlin, was monochromatized by a 3 m normal-incidence monochromator (3m-NIM-2) and focused into the gas cell. A bandwidth of less than 2 meV was achieved with 20 μm entrance and exit slit widths for photon energies around 23.5 eV. This is an improvement by nearly 1 order of magnitude over our previous measurements [9]. The pressure in the differentially pumped target gas cell was kept constant at 0.05 mbar. The undispersed

 0031-9007/97/79(23)/4546(4)$10.00

fluorescence radiation in the wavelength range from 104 nm to about 130 nm was detected directly by a pair of microchannel plates mounted closely outside the LiF window of the gas cell. The exciting-photon energy was varied stepwise in a multiscaling procedure from threshold up to about 300 meV above threshold with a step width of 0.001 nm (corresponding to 0.45 meV). By limiting the investigated energy range to 300 meV no satellites were excited. The investigated Xe II $5s^1 5p^6\, ^2S_{1/2}$ state decays exclusively via two radiative transitions at 110.0 and 124.4 nm [13] into the ionic ground states Xe II $5s^2 5p^5\, ^2P_{1/2,3/2}$. Therefore the $5s$-photoionization cross section of the Xe atom was determined by relating the measured fluorescence intensity (after background subtraction) to the primary photon flux. The energy scale of the exciting radiation was calibrated at the $5s$-electron ionization threshold at 23.397 eV [13] with an estimated uncertainty of less than 1 meV. The absolute values of the photoionization cross section were obtained by normalizing the measured relative cross sections to the absolute value of 0.38 Mb determined at 23.74 eV by Samson and Gardner [14]. Our cross section value at 23.74 eV was obtained through a linear extrapolation of our measured cross sections between 23.62 and 23.67 eV to this energy which appears justified by the fact that no resonances have been observed in this energy region in our work and in [6].

In Fig. 1 the present measurement of σ_{5s} is displayed together with, at the bottom of the figure, the positions of the doubly excited atomic states listed in [6]. The considerable improvement of the resolution with respect to our earlier experiment [9] shows up in clearly resolved structures which display an interesting regularity immediately above threshold. These resonance structures have not been found in the high-resolution photoabsorption measurements [6]. However, their energetic positions turned out to agree rather well with the ones of the f resonances calculated in the hydrogenlike approximation. Therefore, in order to interpret the observed structure in more detail, the following cross section calculations taking into account the strongly delocalized f states were performed.

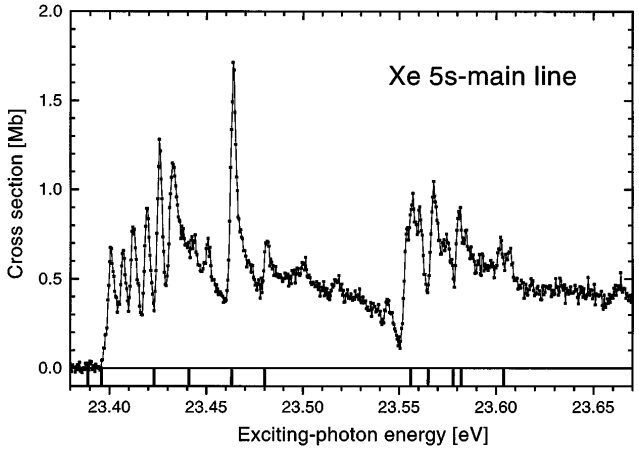

FIG. 1. Xe $5s$-photoionization cross section measured by high resolution PIFS. The positions of resonances measured in photoabsorption [6] have been marked at the bottom.

The partial photoionization cross sections for the following seven channels characterized by the total angular momentum $J = 1$ were calculated: $5p^5_{1/2}\,\epsilon s_{1/2}$, $5p^5_{3/2}\,\epsilon s_{1/2}$, $5p^5_{1/2}\,\epsilon d_{3/2}$, $5p^5_{3/2}\,\epsilon d_{3/2}$, $5p^5_{3/2}\,\epsilon d_{5/2}$, $5s^1_{1/2}$-$\epsilon p_{1/2}$, and $5s^1_{1/2}\,\epsilon p_{3/2}$. Our technique of calculation has been described in detail previously [4,15–17] so that only the general aspects of the technique will be outlined here. The intrashell and intershell correlations connected with $4d$ and $5p$ shells were taken into account using second-order perturbation theory in accordance with Ref. [17]. To calculate the complex structure of the ionic states with the $5s$ vacancy the secular equation technique was used. Basis states $|K\alpha\overline{LSJ}\rangle$ (K is the ionic configuration and $\overline{LSJ}$ are the orbital, spin, and total angular momenta of the state) for the secular equation were $5s^1$, $5p^4\,nd$ ($n = 5, 6, 7, 8, 9$), $5p^4\,ns$ ($n = 6, 7, 8$), $5p^4\epsilon d$ (continuum states with ϵ from 0 to 1500 Ry were taken into account in a quasidiscrete manner [17]).

The calculated ionic eigenvectors were used to construct the basis set for the doubly excited states $|\overline{EJ}nljJ\rangle$. Those ionic states $|\overline{EJ}\rangle$ which have an energy $\leq$5.5 eV above the Xe $5s$ threshold were taken and nl electrons were added to these states ($nl = 6p$, $7p$, $8p$, $9p$, $10p$, $4f$, $5f$, and $6f$). Thus, the total amount of the doubly excited basis states which formed the secular-equation matrix was 225. The following formula was used for the calculation of the diagonal Hamiltonian matrix elements for the doubly excited states energies:

$$\langle \overline{EJ}nljJ|H|\overline{EJ}nljJ\rangle = \overline{E} + \sum_{K\alpha\overline{LS}} \langle K\alpha\overline{LSJ}\,|\,\overline{EJ}\rangle^2 I_K^{nl}\,. \tag{1}$$

I_K^{nl} are the ionization potentials of the nl electron in the K ionic-core configuration calculated with accounting for relativistic and correlational corrections [4,15–17] and $\langle K\alpha\,\overline{LSJ}\,|\,\overline{EJ}\rangle$ are numerical coefficients obtained by solving the secular equation for the ionic states $|\overline{EJ}\rangle$. In Eq. (1) the calculated ionic energies $\overline{E}$ were replaced by the experimental values [13] since the accuracy of the ionic-energy calculation (approximately 80 meV [17]) is not adequate to describe the experimental features with 6 meV spacing (see Fig. 1).

Finally, the cross sections for the photoionization to the Xe II $5s^1_{1/2}$, $5p^5_{1/2}$, and $5p^5_{3/2}$ final states as well as the widths and oscillator strengths characterizing the doubly excited states were calculated as in [4].

The calculated $5s$ and $5p$ cross sections in the $5s$-threshold region were then convoluted with a Gaussian function of 2 meV FWHM representing the primary bandwidth of the ionizing radiation. They are presented in

the upper part of Fig. 2 together with our experimental $5s$ cross section and the positions of the resonances from [6]. For the $5s$ photoionization the theoretical cross section agrees well with the measured one in the lower-energy part. The discrepancies observed in the higher-energy part will be addressed at the end of this paragraph. To understand the origin of the interesting regularily looking structure in the $5s$ cross section near threshold two additional model calculations were made. In the first one the p resonances only were included in the doubly excited states basis set while in the second one the f resonances only were accounted for. The results are presented in the lower part of Fig. 2 where one can see that the p resonances determine the coarse features of the structures in the $5s$ cross section. Contrarily, the f resonances do not manifest themselves independently (see also the lower part of Fig. 2). The reason for this is that nf electrons have large mean radii (namely the mean radius of a $5f$ electron is 31 a.u.) and, simultaneously, a very small density inside the atomic core due to the large centrifugal potential. As a consequence, the f resonances themselves have widths and oscillator strengths which are by 1 to 2 orders of magnitude smaller than the corresponding characteristics of the p resonances. This has been quantified in Table I. Contrarily np electrons, characterizing p resonances, have a considerably larger density inside the atomic core. Nevertheless, the interaction between p and f resonances is not weak because the mean radii of np electrons are also large and their wave functions overlap considerably with those of nf electrons. The admixture of np wave functions to the nf wave functions leads to large changes of the characteristics of the f resonances as documented in Table I. As a result, f resonances become prominent in the $5s$ photoionization cross section. In the higher-energy part, as one can see from Table I, the resonances are associated with the more localized $4f$ electrons which are more strongly influenced by the long-range polarization potential of the ionic core [18] than the delocalized ones. Taking into account this influence in future calculations could reduce the above discrepancy.

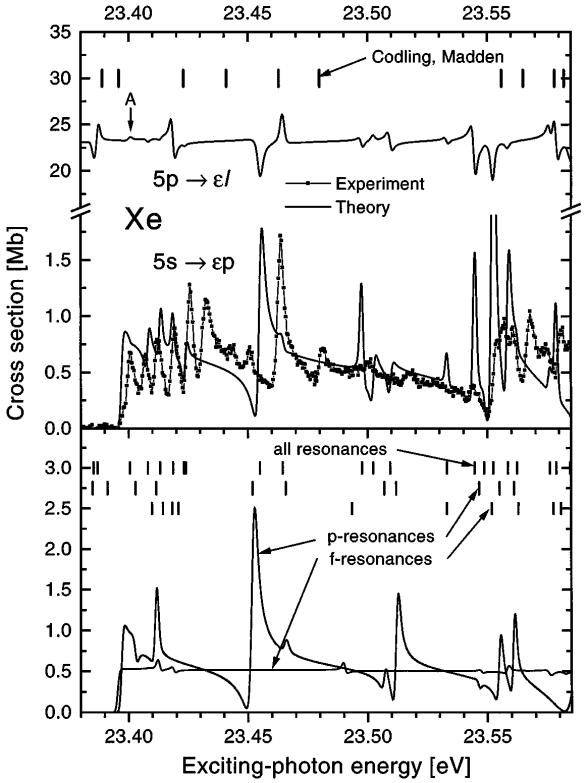

FIG. 2. Upper part: Measured and calculated Xe $5s$-photoionization cross sections near the threshold. The calculated cross sections were convoluted with a Gaussian function of 2 meV FWHM. The total calculated $5p$-photoionization cross section and the positions of resonances measured in photoabsorption [6] are also shown at the top. Lower part: Xe $5s$-photoionization cross sections calculated taking into account either p or f resonances only. The calculated positions of resonances are also shown for each model case separately and after including the interaction between p and f resonances.

In the $5p$ photoabsorption cross section the f resonances are expected to be much less visible and were not observed [6]. This is connected with the decrease of their "contrast" due to large σ_{5p_j} values. An additional reason is that the total $5p$ photoabsorption cross section is a sum of two partial cross sections, namely $\sigma_{5p_{1/2}}$ and $\sigma_{5p_{3/2}}$. Some of the f resonances are of window type in $\sigma_{5p_{1/2}}$ while they are of peak type in $\sigma_{5p_{3/2}}$ or vice versa [10]. As a result, in the total σ_{5p} cross section measured in a photoabsorption experiment like [6] the resulting features are usually less pronounced than in each partial channel. For example, the resonance marked A in Fig. 2 is of window type with an amplitude of 0.5 Mb in $\sigma_{5p_{1/2}}$ while it is of peak type with an amplitude of 0.7 Mb in $\sigma_{5p_{3/2}}$. Hence, in the total σ_{5p} cross section the resulting resonance A is of peak type but with an amplitude of 0.2 Mb only.

It would be possible to observe the f resonances in the partial photoionization cross sections by using photoelectron spectroscopy techniques [10] if an adequate resolution can be attained in the future. At present, the PIFS technique developed by us and applied in this work is the only method with sufficient resolution to separate these resonances and to investigate the effect of strongly delocalized f states on the photoionization process of, e.g., the Xe atom. Moreover, in view of their very small natural widths (no more than a few 10^{-4} eV), the f resonances can be expected to show up even more prominently in future PIFS experiments with further improved resolution.

Financial support from the Deutsche Forschungsgemeinschaft is gratefully acknowledged. The cooperation project of the universities of Kaiserslautern and Rostov-on-Don was funded by the Bundesministerium für Bildung, Wissenschaft, Forschung und Technologie.

TABLE I. Calculated characteristics of some resonances of Xe in the $5s$-threshold region.

Genealogy	Energy (eV)	Percentage with	Percentage without	Oscillator strength (10^{-3}) of pure doubly excited state with interaction of p and f resonances	Oscillator strength (10^{-3}) of pure doubly excited state without interaction of p and f resonances	Width (meV) with	Width (meV) without
Resonances with the p genealogy							
$(^3P)5d\,^4D_{1/2}8p_{3/2}$	23.400	48	39	0.0142	0.0143	0.7267	0.7386
$(^3P)6s\,^2P_{3/2}9p_{1/2}$	23.408	41	48	0.0043	0.0081	0.3128	0.3032
$(^3P)5d\,^2D_{5/2}6p_{3/2}$	23.455	26	29	0.1632	0.2454	1.7913	2.2564
$(^3P)5d\,^4D_{5/2}9p_{3/2}$	23.465	65	75	0.0551	0.0591	1.0094	1.0848
$(^3P)5d\,^4D_{3/2}9p_{1/2}$	23.502	24	26	0.0240	0.0788	0.9402	1.1116
$(^3P)6s\,^4P_{3/2}7p_{1/2}$	23.509	70	40	0.0396	0.0138	0.6983	0.7320
$(^3P)5d\,^4D_{3/2}9p_{3/2}$	23.549	76	93	0.0135	0.0044	0.2872	0.2433
$(^3P)6s\,^2P_{3/2}10p_{3/2}$	23.558	50	35	0.0223	0.0330	0.8947	0.7865
$(^3P)6s\,^2P_{3/2}10p_{1/2}$	23.562	75	70	0.0016	0.0174	0.0595	0.3598
Resonances with the f genealogy							
$(^3P)5d\,^4D_{5/2}5f_{5/2}$	23.413	64	94	0.0055	0.0001	0.1083	0.0439
$(^3P)5d\,^4D_{5/2}5f_{7/2}$	23.419	38	84	0.0533	0.0027	0.2046	0.0738
$(^3P)5d\,^4D_{7/2}5f_{7/2}$	23.423	42	77	0.0029	0.0011	0.3689	0.0623
$(^3P)5d\,^4D_{7/2}5f_{5/2}$	23.424	70	86	0.0045	0.0000	0.1459	0.0109
$(^3P)5d\,^4D_{3/2}5f_{5/2}$	23.498	80	96	0.0390	0.0034	0.1946	0.0913
$(^3P)6s\,^2P_{3/2}6f_{5/2}$	23.533	79	96	0.0092	0.0011	0.0790	0.0517
$(^3P)5d\,^4F_{7/2}4f_{5/2}$	23.545	25	61	0.0825	0.0003	0.4511	0.0612
$(^3P)5d\,^4F_{7/2}4f_{7/2}$	23.552	43	61	0.1394	0.0005	0.8657	0.2523

[1] L. D. Landau and E. M. Lifshitz, *Quantum Mechanics: Non-relativistic Theory* (Pergamon, Oxford, 1977), Chaps. 10 and 11.

[2] K.-H. Schartner, B. Möbus, P. Lenz, H. Schmoranzer, and M. Wildberger, Phys. Rev. Lett. **61**, 2744 (1988).

[3] W. Wijesundera and H. P. Kelly, Phys. Rev. A **39**, 634 (1989).

[4] B. M. Lagutin, V. L. Sukhorukov, I. D. Petrov, H. Schmoranzer, A. Ehresmann, and K.-H. Schartner, J. Phys. B **27**, 5221 (1994).

[5] V. L. Sukhorukov, B. M. Lagutin, I. D. Petrov, H. Schmoranzer, A. Ehresmann, F. Vollweiler, and K.-H. Schartner, J. Electron Spectrosc. Relat. Phenom. **76**, 421 (1995).

[6] K. Codling and R. P. Madden, J. Res. Natl. Bur. Stand. Sect. A **76**, 1 (1972).

[7] H. Schmoranzer, K. Molter, T. Noll, and J. Imschweiler, Nucl. Instrum. Methods Phys. Res., Sect. A **246**, 485 (1986).

[8] A. Ehresmann, F. Vollweiler, H. Schmoranzer, V. L. Sukhorukov, B. M. Lagutin, I. D. Petrov, G. Mentzel, and K.-H. Schartner, J. Phys. B **27**, 1489 (1994).

[9] K-H. Schartner, P. Lenz, B. Möbus, H. Schmoranzer, and M. Wildberger, J. Phys. B **22**, 1573 (1989).

[10] A. A. Wills, A. A. Cafolla, and J. Comer, J. Phys. B **23**, 2029 (1990).

[11] H. Schmoranzer, T. Noll, E. Roueff, H. Abgrall, and R. J. Bieniek, Phys. Rev. A **42**, 1835 (1990).

[12] E. Flemming, O. Wilhelmi, H. Schmoranzer, and M. Glass-Maujean, J. Chem. Phys. **103**, 4090 (1995).

[13] J. E. Hansen and W. Persson, Phys. Scr. **36**, 602 (1987).

[14] J. A. R. Samson and J. L. Gardner, Phys. Rev. Lett. **33**, 671 (1974).

[15] H. Schmoranzer, A. Ehresmann, F. Vollweiler, V. L. Sukhorukov, B. M. Lagutin, I. D. Petrov, K.-H. Schartner, and B. Möbus, J. Phys. B **26**, 2795 (1993).

[16] V. L. Sukhorukov, B. M. Lagutin, I. D. Petrov, H. Schmoranzer, A. Ehresmann, and K.-H. Schartner, J. Phys. B **27**, 241 (1994).

[17] B. M. Lagutin, I. D. Petrov, V. L. Sukhorukov, S. B. Whitfield, B. Langer, J. Viefhaus, R. Wehlitz, N. Berrah, W. Mahler, and U. Becker, J. Phys. B **29**, 937 (1996).

[18] T. N. Chang, J. Phys. B **8**, 743 (1975).